Application of the Global Optimization Approaches to Planar Near-Field Antenna Phaseless Measurements

Jan PUSKELY, Zdeněk NOVÁČEK

Dept. of Radio Electronics, Brno University of Technology, Purkyňova 118, 612 00 Brno, Czech Republic

xpuske01@stud.feec.vutbr.cz, novacek@feec.vutbr.cz

Abstract. *This paper deals with a method of the radiation pattern determination of the directional antennas. The method combining both the functional minimization method and the Fourier iterative algorithm is based on the phaseless near-field measurement on two plane surfaces. The method is used for a reconstruction of the phase distribution on the aperture of the measured antenna, and for the determination of the antenna radiation pattern, consequently. The binary genetic algorithm (BGA), the real-valued genetic algorithm (RVGA), the particle swarm optimization (PSO), and differential evolutionary algorithm (DEA) were chosen for the global functional minimization. The paper is aimed to analyze the performance of the global optimizations (GOs) when solving the described problem, and to compare the GOs. GOs were examined through data achieved by measurement of a horn antenna and a parabola.*

Keywords

Radiation pattern, planar near-field scanning, particle swarm optimization (PSO), binary genetic algorithms (BGA), real-valued genetic algorithm (RVGA), differential evolutionary algorithm (DEA), Fourier iterative algorithm.

1. Introduction

When dealing with a near-field to far-field (NF-FF) transformation for an antenna measurement, traditional techniques require not only the amplitude but also the phase information of the NF data in order to calculate accurately the far-field pattern of the antenna under test (AUT). However, obtaining the complex (amplitude and phase) values of the electric field intensity at millimeter-wave frequencies is difficult. At low frequencies, the amplitude-only measurement techniques are economical to employ. These reasons are often the motivations of studying techniques that allow the calculation of the FF pattern from amplitude measurements in the NF.

In this paper, a method applicable to computing FF antenna patterns from NF phaseless measurements on two plane surfaces placed in different distances form antenna aperture is presented. The method is based on the reconstruction of the complex intensity of an electric field distribution on the measured antenna aperture from the measured amplitudes, and the determination of the antenna radiation pattern consequently (shown in Fig. 1).

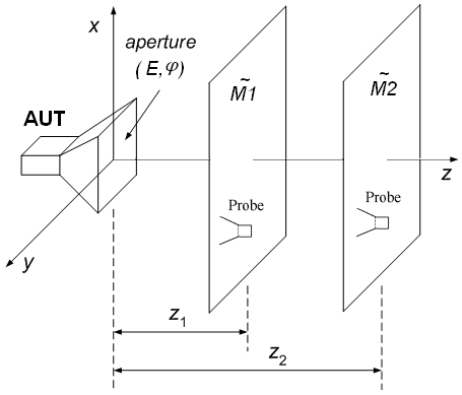

Fig. 1. The principle of the NF antenna phaseless measurement.

For the reconstruction of the phase distribution, two methods are exploited, the functional minimization method [1] and the Fourier iterative algorithm (FIA) [2].

In our case, the binary genetic algorithm (BGA), the real-valued genetic algorithm (RVGA), the particle swarm optimization (PSO) and differential evolutionary algorithm (DEA) (used in [11]) were chosen for the functional minimization. The paper originality is in the application and comparison of four different global optimization methods (BGA, RVGA, PSO, DEA) to find the initial estimation in the area of the global minimum.

Their comparison was carried out on the radiation pattern reconstruction of the horn antenna and the parabola. Since the global optimization does not reach accurate results in a given time, we use them to find an initial estimation only. For faster revealing of the global minimum area, this paper considers also possibilities of accelerating the GOs.

The achieved initial estimation is improved by the second mentioned method, Fourier iterative algorithm (the local method). In the paper, a method combining both the functional minimization and the Fourier iterative algorithm is described [3], [11].

2. Phase Reconstruction Method

The functional minimization method is based on the minimization of the difference between the calculated amplitudes and measured ones on two plane surfaces in the near-field region. Revealing the minimal function representing the complex intensity of the electric field distribution on the aperture of the measured antenna is our goal. If the phase distribution on the aperture is known, we are able to determine both the phase distribution on two scanning planes and the antenna radiation patterns.

The algorithm of the functional minimization assumes knowledge of the amplitudes on two plane surfaces at least, scanning planes distances from the AUT and dimensions of the AUT.

The used method can exploit local optimization techniques or global ones. At the present, the functional minimization is mainly based on the local minimization methods (the Newton method, e.g.). In general, both a global minimum and a few local minima can be revealed when searching for minima of the functional. The number of local minima increases with an increasing error of measured amplitudes. Thus the local minimization can be used in case of choosing an initial estimation in the area of the global minimum only or in case of an adjusted functional without local minima [1], [4].

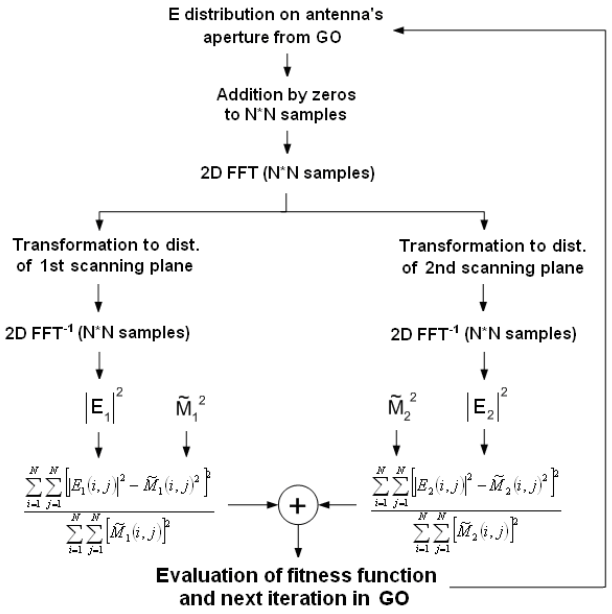

Fig. 2. The flow chart of minimizing algorithm by global optimization (GO).

Global optimization techniques are very useful in electromagnetic issues, when searching for the global maximum (minimum) in a multidimensional domain. In contrast to the local minimization, the use of the global algorithm is not conditioned by any choice of the initial estimation and an additional modification of the minimized functional. On the other hand, the convergence can slow down.

The difference between the local approach which is used for the minimization of the functional in [1] and the global one consists in the fact that error distributions calculated in distances of scanning planes are transformed back into the plane of the measured antenna aperture in case of minimizing the functional. The method requires moreover executing four Fourier transformations and two multiplications. Thus, using the global algorithm leads moreover to the reduction of the CPU-time required for evaluating the objective function and to the acceleration of the process. The flow chart of the minimizing algorithm is shown in Fig. 2.

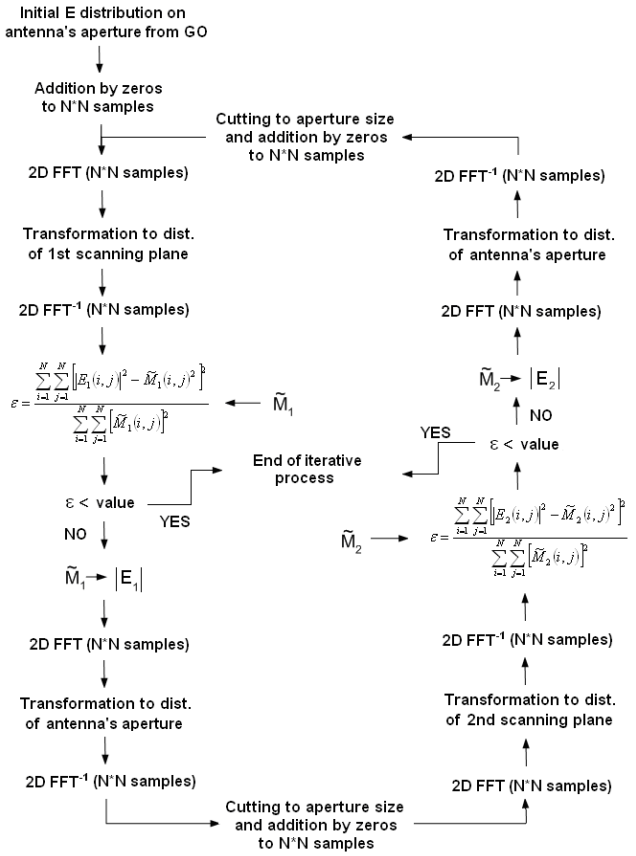

Fig. 3. The flow chart of the Fourier iterative algorithm.

The second part consists of the Fourier iterative algorithm [2] which also minimizes the functional. The flow chart of the Fourier iterative algorithm is shown in Fig. 3. The initial estimation achieved by the functional minimization method is refined in every step. The whole cycle is finished if the difference between the actual value and the previous one is smaller than the defined value or if the difference between the measured amplitudes and the estimated ones is better than the required accuracy. The iterative algorithm is simpler and more straightforward against the method of the functional minimization. On the other hand, the convergence can be slower compared to the numerical methods. A success of the Fourier iterative algorithm as well as other local methods depends on the choice of the initial estimation. Thus, the method is suitable for our case.

The functional F which is minimized by both the algorithms is of the following form:

$$F = \frac{\sum_{i=1}^{N}\sum_{j=1}^{N}\left[\left|E_1(i,j)\right|^2 - \tilde{M}_1(i,j)^2\right]^2}{\sum_{i=1}^{N}\sum_{j=1}^{N}\tilde{M}_1(i,j)^2} + \frac{\sum_{i=1}^{N}\sum_{j=1}^{N}\left[\left|E_2(i,j)\right|^2 - \tilde{M}_2(i,j)^2\right]^2}{\sum_{i=1}^{N}\sum_{j=1}^{N}\tilde{M}_2(i,j)^2}. \quad (1)$$

In (1), $E_1(i, j)$ is the computed complex intensity in the point i, j on the first scanning plane, and $E_2(i, j)$ is the computed complex intensity in the point i, j on the second scanning plane. Next, $\tilde{M}_1(i,j)$ is the measured amplitude in the point i, j on the first scanning plane, and $\tilde{M}_2(i,j)$ is the measured amplitude in the point i, j on the second scanning plane.

The presented method eliminates all the hereinbefore disadvantages. The method combines the global optimization and the Fourier iterative algorithm [3]. First, the algorithm is used to find an initial estimation lying in the area of the global minimum. The second part consists of the common Fourier iterative algorithm improving the initial estimation.

2.1 Global Optimization: BGA, R-VGA , PSO and DEA

Four global optimizations were chosen for the functional minimization: the binary genetic algorithm (BGA), the real-valued genetic algorithm (RVGA), the particle swarm optimization (PSO), and the differential evolutionary algorithm (DEA).

2.1.1 Particle Swarm Optimization

The PSO algorithm emerges as a powerful stochastic optimization method inspired by the social behavior of organisms such as bird flocking or fish schooling, in which individuals have memory and cooperate to move towards a region containing the global or a near-optimal solution [5]. The PSO is exploited to solve a multi-dimensional discontinuous problem. Concretely, the swarm moves in a 390-dimensional space (390 real unknowns). The solution space is bordered from $-\pi$ to $+\pi$ in case of phases and from zero to an existing maximal value on the first sampling plane in case of amplitudes.

The algorithm is initialized by an initial random distribution of the swarm and by searching the personal minimum p_{best} and the global minimum g_{best} in the given space. The position of the global minimum and the personal one are used to determine an optimal velocity operator (the direction and the speed of flight) of the agents to the area of best solutions in the next iteration [5]. For updating the velocity operators, we applied the following formulas [6]:

$$\mathbf{v}_n = K\left[\mathbf{v}_n + \varphi_1 r_1\left(\mathbf{p}_n - \mathbf{x}_n\right) + \varphi_2 r_2\left(\mathbf{g}_n - \mathbf{x}_n\right)\right], \quad (2)$$

$$\mathbf{x}_n = \mathbf{x}_n + \Delta t\,\mathbf{v}_n . \quad (3)$$

Here, $\mathbf{v}_n$ is the velocity vector of the nth agent, $\boldsymbol{x}_n$ denotes the position of the nth agent, $\mathbf{p}_n$ is the position of the personal optimum of the nth agent, and $\mathbf{g}_n$ is the position of the global optimum of the whole swarm. Next, r_1 and r_2 are random numbers from 0 to 1, the factor K is known as a restriction factor, φ_1 and φ_2 are the acceleration constants. PSO exhibits the best convergence properties if the restriction factor is chosen 0.729 and acceleration constants equal to 2.4 and 1.7, respectively [3], [9]. If a new velocity vector of the agent is known, its new position can be computed by (3) where Δt is a time step usually chosen to be one. Otherwise, the algorithm shows the best properties when absorbing walls were chosen as the border condition, and the swarm consisted of 30 agents [3].

2.1.2 Genetic Algorithms

By analogy with natural selection and evolution, the set of parameters to be optimized (genes) defines an individual (chromosome). The set of individuals forms the population, which is evolved by means of the selection, the crossover, and the mutation genetic operators [7]. In this paper, two GA-based schemes have been investigated and implemented: classical binary encoding [7, 8] and real-valued GA [8].

In the case of the binary GA, thirty individuals were chosen to form a population. Each individual (chromosome) consisted of binary genes by 8 bits. The elitist strategy was taken into account. Half best individuals were propagated unchanged. The tournament was used for selecting parents. Parents were obtained by two rounds selection and were sorted by fitness function. Parents were selected to make 14 new offspring by the uniform crossover and the five new offspring were created by the mutation of the remained parents. 15 best offspring from this group completed the elitist. The probability of crossover was set to p_c = 70 %, and the probability of mutation to p_m = 25 %.

In the case of the real-valued GA, the number of bits required to accurately encode a parameter does not need to be considered. Instead, the amplitudes and phases are encoded in terms of real numbers in between the given bounds. The number of chromosomes was set to 24 in the initial population. The tournament selection was the best selection strategy, and the linear crossover was the selected crossover strategy. In this case, three offspring are generated from two chosen parents by following formulas [8]:

$$p_{new1} = 0.5p_{mn} + 0.5p_{dn}, \quad (4a)$$

$$p_{new2} = 1.5p_{mn} - 0.5p_{dn}, \quad (4b)$$

$$p_{new3} = -0.5p_{mn} + 1.5p_{dn} \quad (4c)$$

where p_{mn} is the nth parameter in the mother chromosome and p_{dn} is the nth parameter in the father chromosome. Any parameter outside the bounds is discarded in favor of the other two ones. Then, the best two offspring are chosen to propagate.

12 parents were chosen by the tournament selection to make 12 offspring by the linear crossover and the last two offspring were created by the mutation of two random parents. These 14 new individuals completed 10 elitist individuals. The probability of the crossover was set to $p_c = 100$ %, and the probability of the mutation to $p_m = 25$ % [13].

2.1.3 Differential Evolutionary Algorithm

Differential Evolution algorithm (DEA) is a new heuristic approach which works with real numbers as well as RVGA [12]. The DE algorithm is a population based algorithm like genetic algorithms using the similar operators; crossover, mutation and selection. The main difference is that genetic algorithms rely on crossover while DEA relies on mutation operation.

DEA is a parallel direct search method which utilizes NP (number of the individuals in population) D-dimensional parameter vectors $x_{i,G}$, i = 1, 2, 3, …, NP as a population for each generation G. DEA generates new parameter vectors by adding the weighted difference between two population vectors to a third vector (5). This operation is called mutation. The mutated vector's parameters are then mixed with the parameters of another predetermined vector, the target vector, to yield the so-called trial vector. Parameter mixing is often referred to as "crossover".

For each target vector $x_{i,G}$, i = 1, 2, 3, …, NP, a mutant vector is generated according to [12]

$$v_{i,G+1} = x_{r1,G} + F \cdot (x_{r2,G} - x_{r3,G}) \tag{5}$$

where i, $r1$, $r2$, $r3 \in \{1, 2, \ldots, NP\}$ are randomly chosen and must be different from each other. In (5), F is the scaling factor $\in (0, 2)$. The parent vector is mixed with the mutated vector to produce a trial vector $u_{ji,G+1}$ [12]

$$u_{ji,G+1} = \begin{cases} u_{ji,G+1} & \text{if } (rand_j \le CR) \text{ or } j = rn_i \\ x_{ji,G} & \text{if } (rand_j > CR) \text{ and } j \ne rn_i \end{cases} \tag{6}$$

where j = 1, 2, …, D; $rand_j \in |0,1|$ is the random number; CR is crossover constant $\in |0,1|$ and $rn_i \in (1,2,\ldots D)$ is the randomly chosen index. If the trial vector yields a lower cost function value than the target vector, the trial vector replaces the target vector in the following generation. This last operation is called selection.

The parameters of the DEA used for evaluating new member were chosen similar to those used in [11]. Thus, for our specific case, we have used these parameters: the probability of the mutation in mutant vector p_m = 0.1, the crossover rate CR = 0.9 and the scaling factor F = *rand*. In [11], the scaling factor was set on value 1.2 but we weren't able to find the global minimum area in this case. The number of population NP was chosen 24.

In short, the PSO, RVGA and DEA algorithms require fewer lines of code than BGA and are easier to implement. Moreover, PSO and DEA against GAs have a small number of the parameters to be tuned. In PSO, the population size, the restriction factor and the acceleration constants and in DEA, number of population, scaling factor and crossover rate summarize the parameters to be selected and tuned, whereas in GAs the population size, the selection, the crossover and mutation strategies, as well as the crossover and mutation rates influence the results.

3. Comparison of GO Algorithms

In this section, the comparison of the global optimization approaches is presented. Their comparison was carried out on the radiation pattern reconstruction of the horn antenna and parabola. Data used for analysis were available from [3].

The horn antenna T1-R100 had the aperture of the size 136×101 mm and the horn length of 173 mm. The antenna was analyzed at the frequency 12.4 GHz. The measurement site is shown in Fig. 4. The horn antenna was attached to the tripod so that the longer site of the antenna aperture was parallel to the horizontal plane (H polarization). The scanning probe (the waveguide R100 aperture) was oriented horizontally, too.

Fig. 4. The measurement site arrangement.

The values of the horizontal electric field intensity component in discrete points placed in the vertical direction and the horizontal one with the pitch of 10 mm (0.41λ) at two scanning planes of the size 400×400 mm were measured by a probe. Generally, 1681 (41×41) values on each plane were achieved. The measurement was per-

formed in the Rayleigh zone. The first plane was placed in the distance of 60 mm (~2.48λ) and the second one in the distance of 70 mm (~2.89λ) (the distance was measured from the antenna aperture to the waveguide aperture). Due to the arrangement of the measurement, the valid angle is $\theta_v = 62^o$**.** Since the aperture of the antenna is 136×101 mm (15 times 13 sampling points), the solution space contains 390 real parameters which optimal values are going to be found out.

The second data were from measurement of the parabola with reflector diameter of 0.6 m. The spacing of discrete points was also 10 mm and the scanning planes had the size of 800×800 mm. The first plane was placed in the distance of 268 mm (~12.86λ) and the second one in the distance of 298 mm (~14.3λ). These distances correspond to the valid angle $\theta_v = 18.55^o$**.** The waveguide R140 was used as a scanning probe. The antenna was analyzed at the frequency 14.4 GHz. The number of scanning points was 81×81 and the solution space contains 5202 real parameters.

The configuration of the optimization schemes considered in the analysis is summarized in Tab. 1 and was selected according to the results of a preliminary parametric study carried out individually with each algorithm [3], [9], [10], [11], [13]. Each optimization was repeated 10 times and was stopped in the 5000th iteration. The averaged realizations are shown in Fig. 5a for the case of the horn antenna and in Fig. 5b for the case of the parabola.

Optimization algorithm	Parameters
Real-Valued GA	**Tournament selection; linear crossover $P_C = 1$; random mutation $P_m = 0.25$; elitism; $PS = 24$**
Binary GA	**Tournament selection; uniform crossover $P_C = 0.7$; random mutation $P_m = 0.25$; elitism; $PS = 30$; 8 bits to encode**
PSO	**Constant inertia: K =0.729, $\varphi_1 = 1.4$, $\varphi_2 = 2.4$; absorb wall; $PS = 30$**
DEA	**$p_m = 0.1$; $CR = 0.9$; $F = 1.2$; $PS = 24$**

Tab. 1. Settings of the optimization algorithms.

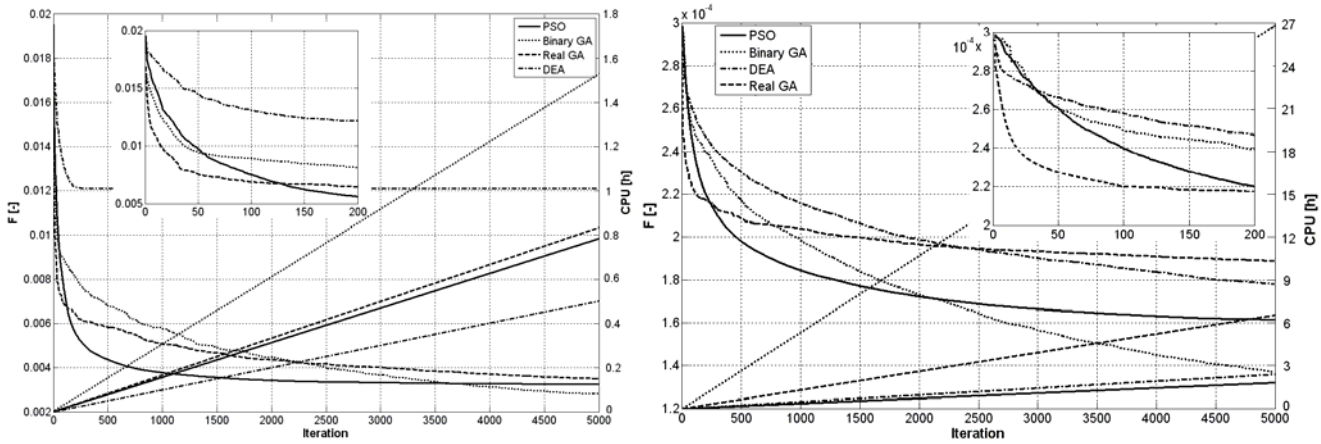

Fig. 5. Convergence behavior of the optimization algorithms; a) for case of the horn antenna ; b) for case of the parabola; averaged results for 10 independent runs carried out with each method.

Obviously from Fig. 5a (390 parameters were optimized), the convergence of the genetic algorithms (GAs) and DEA is less declivitous against the particle swarm optimization (PSO) but all optimizations reach approximately similar global minimum values except DEA after 5000 iteration steps. In the case of DEA, the fitness functions don't reach such the global minimum values as other optimizations and begin to stagnate from about 200 iteration steps. In the case of GAs, the objective functions still fall slowly down in contrast to PSO where the fitness function almost stagnates from about 2000 iteration steps, and is already without any significantly change.

Clearly from Fig. 5b (5202 parameters were optimized), the BGA has the best convergence properties; while the RVGA has the worst ones. It is noteworthy that none of the optimization techniques stagnates after the 5000 iteration. Concerning the computational costs of each optimization scheme, Fig. 5 shows the average CPU-time required by each method. Results demonstrate the superiority of PSO, RVGA and DEA, which saves up to 50% of the CPU-time with regard to BGA in the cases when we optimized less number of variables. With an increasing number of the variables, the demand on the CPU-time increases especially in the cases of GAs.

Otherwise, the real-valued genetic algorithm (RVGA) converges very quickly to the solution in the initial phase in both cases and only PSO which exhibits the best performance exhibits a comparable behavior as RVGA. Thereinafter, the RVGA can demonstrate the ability to find the global minimum area quickly among of all optimizations.

3.1 Results of the NF-FF Transformation Achieved by Global Approaches

All the optimizations were used for the initial reconstruction of the phases and amplitudes on the antenna aperture and the scanning planes (phases only), respectively.

The far-field results obtained by the optimization schemes are shown in Fig. 6 and 7. Fig. 6 shows radiation pattern results obtained after 150, 500 and 3000 iteration of the optimization schemes for case of the horn antenna, and Fig. 7 shows results for case of the parabola.

Obviously from Fig. 6, only RVGA and PSO reached the area of the global minimum after 150 iterations since the reconstructed radiation patterns match to the theoretical radiation patterns after applying FIA for case of the horn antenna (390 optimized parameters).

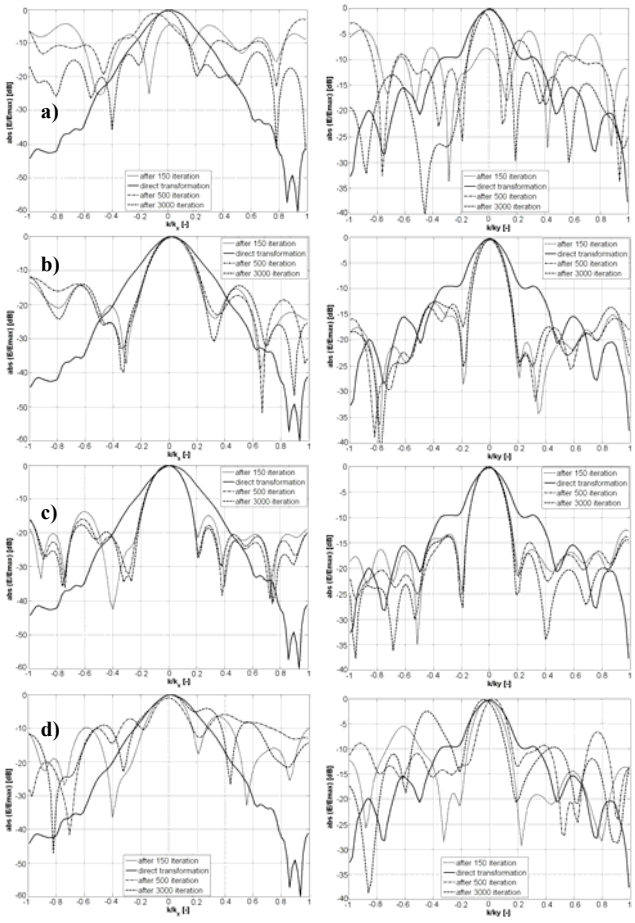

Fig. 6. Reconstructed H plane (left side) and E plane (right side) radiation patterns of the horn antenna after appplying: a) BGA; b) RVGA; c) PSO; d) DEA.

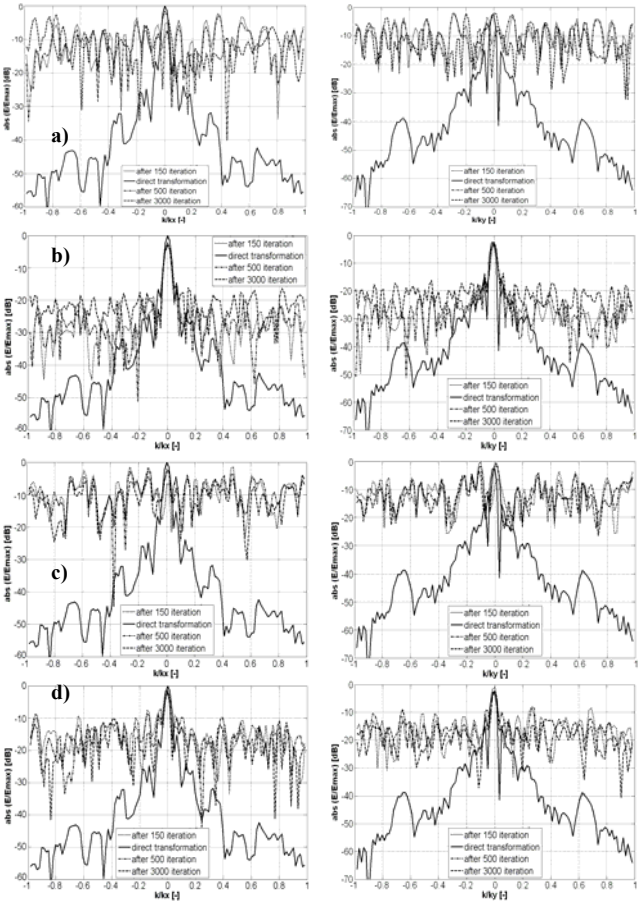

Fig. 7. Reconstructed H plane (left side) and E plane (right side) radiation patterns of the parabola after appplying; a) BGA; b) RVGA; c) PSO; d) DEA.

DEA is also able to find the global minimum area after 150 iterations but the solutions are unstable. In comparison with the results in [11] where the global minimum was found after several tens of iterations, we weren't sometimes able to reach the global minimum even after 5000 iterations. This is probably due to choice of another minimizing functional. BGA has similar features as DEA. The solutions achieved after applying BGA are also unstable i.e. don't lie in the area of the global minimum. Certainty of the estimation lying in the area of the global minimum is obtained after about 3000 iteration [10].

GOs applied to the measurement data of the parabola just confirmed perfect properties of the RVGA (Fig. 7). Thus, RVGA surpasses other optimizations by the ability of finding the area of the global minimum in an extremely short time although it doesn't exhibit the best convergence properties.

3.2 Influence of Different Spacing between Scanning Planes

In case of the horn antenna, the values of the horizontal electric field intensity component were available on three planes at the frequency 12.4 GHz. The scanning planes were placed in the distances of 50 mm, 60 mm and 70 mm. Analysis were carried out for all optimizations.

Each optimization was repeated 10 times and was stopped in the 5000th iteration. Influence of the different spacing between the scanning planes is shown in Fig. 8.

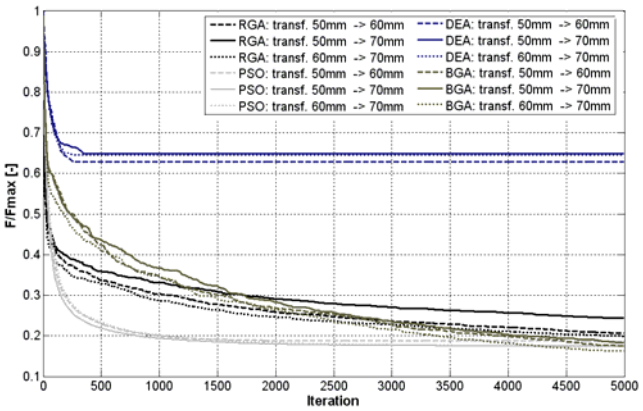

Fig. 8. Influence of the different spacing between the scanning planes.

In the case of BGA, PSO and DEA, obviously, the different spacing between the scanning planes doesn't substantially affect the convergence properties. On the other hand, in case of RGA, the convergence speed in the scheme using transformation between planes distant from each other 10 mm is better than in case where the planes are separated by a distance 20 mm. Therefore, it is better for given setting RGA when the both scanning planes will be closer to each other.

Due to we have available data only on three planes it is difficult to generalize these findings. The influence of the different spacing between the scanning planes will be monitored closely in the next part of the research.

3.3 Acceleration of GO Convergence Speed

Since the convergence speed of the global optimizations is very slow in the case of the random initial estimation, the limited knowledge of the phase on the antenna aperture and the uniform phase distribution were considered. The phase distribution on the antenna aperture was obtained by transforming the known phase distribution with a given accuracy from the first scanning plane. The phase accuracies on the first scanning plane were chosen ±5°, ±30° and ±90°.

The optimizations were repeated 10 times for the different knowledge of the phase on the antenna aperture and were stopped in the 1000th iteration. The averaged realizations are shown in Fig. 9.

Fig. 9 shows that knowledge of the phase distribution with various accuracies on the antenna aperture influences the convergence speed and reached objective function value. In the case of PSO and RVGA, the convergence curves are comparable with the random estimation whereas in the case of BGA and DEA, the influence of the phase knowledge is noticeable. Notice that all convergence curves have the similar progress regardless of the phase accuracy on the antenna aperture except DEA.

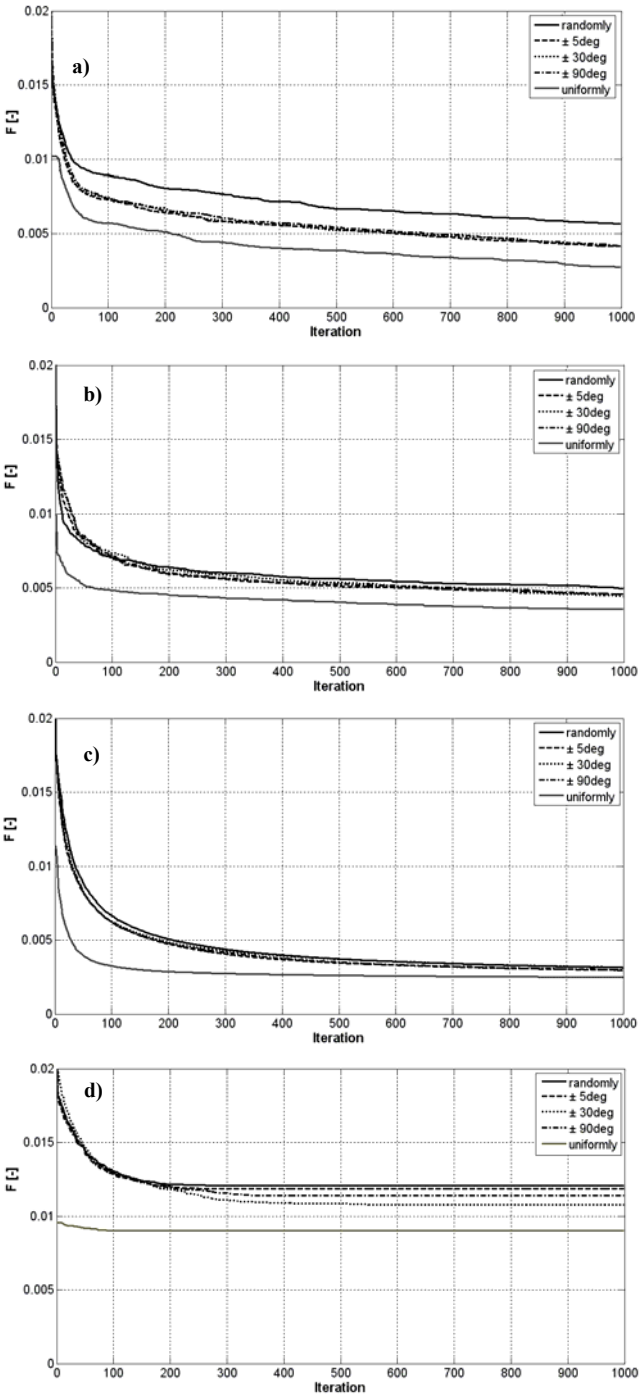

Fig. 9. Comparison of the random estimation, the uniformly estimation and the estimation with various knowledge of the phase on the antenna aperture; a) BGA; b) RVGA; c) PSO; d) DEA.

Comparison of the random estimation and the estimation with uniformly selected phase distribution on the antenna aperture is also shown in Fig. 9. The uniform phase distribution means that the constant phase distribution is chosen on the whole antenna aperture. The phase is divided uniformly according to the number of the agent in the swarm and the number of the chromosome, respectively. The uniform phase distribution achieves better objective functions than random estimation whereas the improvement is noticeable in the case of GAs. Compared to the

random estimation, the convergence curves decrease almost twice quickly and reach twice smaller objective function value. Let us emphasize that the convergence speed depends on the type of the given antenna in the case of the uniformly phase distribution.

4. Results of the NF-FF Transformation

All the optimizations were used for the initial reconstruction of the phases and amplitudes on the antenna aperture and the scanning planes (phases only), respectively.

Fig. 6 and 7 show the radiation patterns which are achieved after GOs from the random initial estimation. The reconstructed far-field radiation patterns show that any of these optimizations has not achieved accurate results yet, and the Fourier iterative algorithm has to be applied to ensure the required precision of the radiation patterns. The far-field results obtained by the optimization schemes and the Fourier iterative algorithm (FIA) are shown in Fig. 10 and 11.

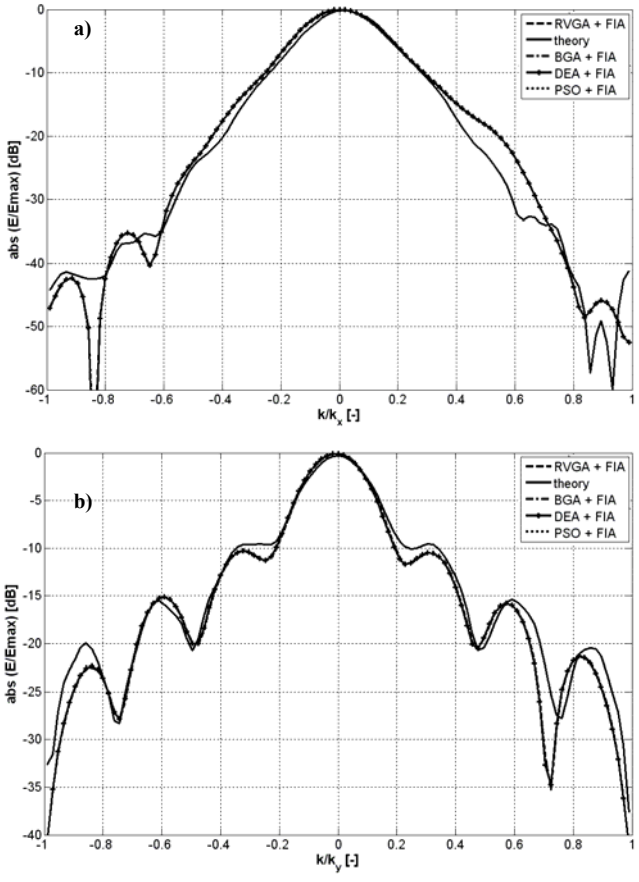

Fig. 10. The reconstructed radiation patterns of the horn antenna after applying GOs +FIA; a) H plane; b) E plane.

In the case of the horn antenna, the reconstructed radiation patterns obtained by the FIA are almost identical with the courses gained by the direct transformation. This illustrates the correct result, thus finding a global minimum. In the case of the parabola, the reconstructed radiation patterns are in good agreement with the direct transformation only in cases of the initial estimations obtained by PSO and RVGA. In the case of PSO, the initial estimate was obtained after about 20 thousand iteration (convergence has stagnated). The estimate achieved by RVGA was stopped after about 10 thousand iterations.

As shown in Fig. 11, FIA has not been able to reconstruct the radiation patterns of the parabola from the initial estimate achieved by the DEA and the BGA, even after 30 thousand iterations.

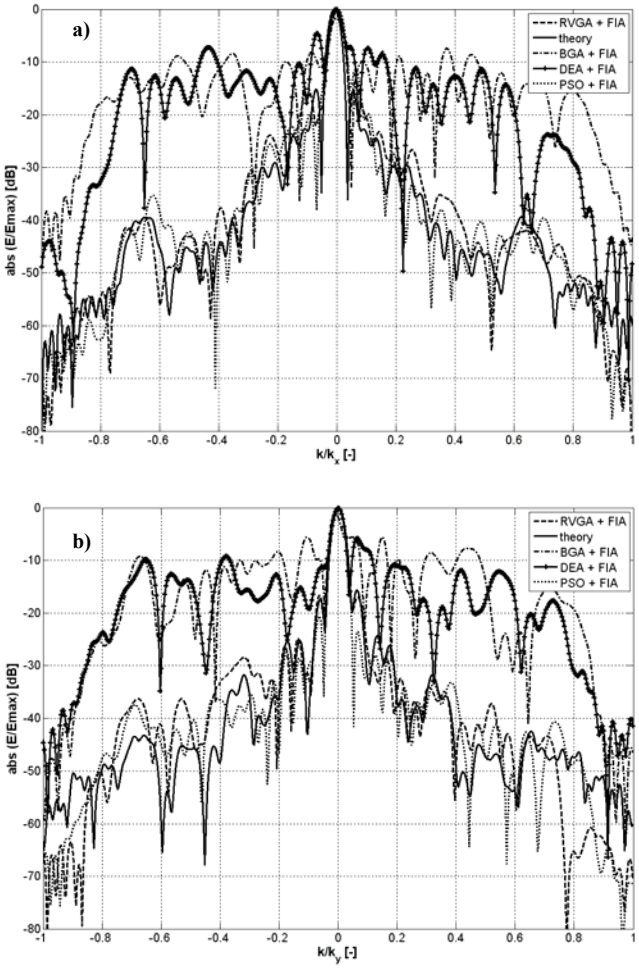

Fig. 11. The reconstructed radiation patterns of the parabola after applying GOs + FIA; a) H plane; b) E plane.

Thus, on the basis of the achieved results, we can conclude that all optimizations are able to reach the global minimum in the cases of relatively small number of the variables. But only PSO and RVGA passed in the cases of the large number of the optimized variables. PSO with given parameters exhibits better convergence properties than other optimizations but RVGA is able to find the area of the global minimum in a shorter time than PSO. From this view, DEA and BGA have worse properties.

The limited knowledge of the phase on the antenna aperture and the uniform phase distribution noticeably affect the convergence acceleration of the minimization

algorithm in the case of DEA, BGA and RVGA, and lesser in the case of PSO. Moreover, it was found out that for given setting of the RVGA, the convergence has better properties when the both scanning planes will be closer to each other.

PSO and DEA are easier to tune and implement than GAs. The CPU-time demands of PSO and DEA are comparable and in comparison with the GAs are smaller. PSO and RVGA seem to be the suitable tool to solve the problem for the ability of finding the area of the global minimum in a short time.

5. Conclusion

GAs, PSO and DEA were compared, their pros and cons investigated and reported when used as a part of the method that uses amplitudes on two scanning planes in the near zone of the antenna for the reconstruction of the antenna radiation patterns.

All mentioned optimizations were demonstrated to be the efficient tool for minimizing complicated multi-dimensional discontinuous problems. PSO and RVGA surpass DEA and BGA by the ability of finding the area of the global minimum in a shorter time. That's why they seem to be the suitable tool for our problem.

Associating the global algorithms and the Fourier iterative algorithm, we obtain a procedure which is able to reconstruct radiation patterns from the random initial estimation.

Acknowledgements

The research described in this contribution was financially supported by the Czech Grant Agency under the grants no. 102/07/1084 and 102/08/H018, and by the research program MSM 0021630513: Advanced Communication Systems and Technologies. The research is a part of the COST project IC0603 ASSIST.

References

[1] BUCCI, O. M., D'ELIA, G., LEONE, G., PIERRI, R. Far-field pattern determination from the near-field amplitude on two surfaces. *IEEE Transaction on Antennas and Propagation*. 1990, vol. 38, no. 11, p. 1772–1779.

[2] YACCARINO, R. G., RAHMAT-SAMII, Y. Phaseless bi-polar planar near-field measurements and diagnostics of array antennas. *IEEE Transactions on Antennas and Propagation*. 1999, vol. 47, no. 3, p. 574–583.

[3] TKADLEC, R. *Near-Field Antenna Measurements. Dissertation Thesis.* Brno: Brno University of Technology, 2005.

[4] ISERNIA, T., LEONE, G., PIERRI, R. Radiation pattern evaluation from near-field intensities on planes. *IEEE Transactions on Antennas and Propagation*. 1996, vol. 44, no. 5, p. 701 – 710.

[5] ROBINSON, J., SINTON, S., RAHMAT-SAMII, Y. Particle swarm, genetic algorithm, and their hybrids: optimization of a profiled corrugated horn antenna. In *Proceedings of the IEEE International Symposium on Antennas and Propagation*. San Antonio: IEEE, 2002, vol. 1, p. 314–317.

[6] CARLISLE, A., DOIZIER, G. An off-the-shelf PSO. In *Proc. Workshop Particle Swarm Optimization*. Indianapolis (USA), 2001.

[7] JOHNSON, J. M., RAHMAT-SAMII, Y. Genetic algorithms in engineering electromagnetics. *IEEE Antennas and Propagation Magazine*. 1997, vol. 39, no. 4, p. 7–21.

[8] HAUPT, R. L., HAUPT, S. E. *Practical Genetic Algorithm*. A Wiley-Interscience Publication, 1998, ISBN 0-471-18873-5.

[9] PUSKELY, J., NOVÁČEK, Z., POKORNÝ, M. Using global optimization approaches to reconstruct radiation patterns. In *Proceedings of the 14th Conference on Microwave Techniques Comite 2008*. 2008, p. 347-350. ISBN 978-1-4244-2137-4.

[10] PUSKELY, J., NOVÁČEK, Z. Application of the global optimization approaches to planar near-field antenna phaseless measurements. In *Proceedings MMS'2008 Mediterranean Microwave Symposium*. Damascus (Syria), 2008, p. 231-236. ISBN 9954-8577-0-2.

[11] RAZAVI, S. F., RAHMAT-SAMII, Y. A new look at phaseless planar near-field measurements: limitations, simulations, measurements, and a hybrid solution. *IEEE Antennas and Propagation Magazine*, 2007, vol. 49, no. 2, pp. 170-178.

[12] ZELINKA, I. Artificial Intelligence in Problems of Global Optimization. Prague: BEN, 2002, 190 p. ISBN 80-7300-069-5.

[13] PUSKELY, J., NOVÁČEK, Z. Antenna far-fields determination from phaseless measurement using the real-valued GA. In *Proceedings of the Junior Scientist Conference 2008*. Vienna, 2008, p. 271 - 272. ISBN 978-3-200-01612-5.

About Authors...

Jan PUSKELY was born in Přerov, Czech Republic, in 1982. He received his master's degree in Electrical Engineering from the Brno University of Technology in 2007. At present, he is a PhD student at the Department of Radio Electronics, Brno University of Technology. His research interest is focused on radiation and propagation of electromagnetic waves and near fields of antennas.

Zdeněk NOVÁČEK was born in Kamenná, Czech Republic, in 1945. He received his master's degree in 1969 and CSc. (PhD) degree in 1980, both from the Brno University of Technology. Since 1969, he has been working as Senior lecturer and since 1997 as Associated Professor at the Department of Radio Electronics, Brno University of Technology. His research interests are focused on the theory of electromagnetic field, antennas and propagation of radio waves, mobile antennas, antenna measurements and the space-time signal processing.